JACS
JOURNAL OF THE AMERICAN CHEMICAL SOCIETY

COMMUNICATION

pubs.acs.org/JACS

On Understanding Stacking Fault Formation in Ice

Payman Pirzadeh and Peter G. Kusalik*

Department of Chemistry, University of Calgary, Calgary, Alberta, Canada T2N 1N4

Supporting Information

ABSTRACT: Despite dedicated efforts aimed at revealing possible molecular structures of the ice defects associated with stacking faults in ice (I), these molecular arrangements have remained a puzzle. Here we demonstrate how the reorganization of water molecules on different faces of ice (I) can facilitate formation of stacking faults within a crystal. We show that a pair of point defects can manifest a particular combination of coupled five- and eight-membered rings (5−8 rings). These structural motifs can facilitate a shift in layers within an ice (I) crystal, thereby inducing stacking faults. Furthermore, the presence of molecular solutes such as methane at the ice interface appears to trigger the formation of coupled 5−8 rings. The observation of such coupled 5−8 ring defects provides insights into the possible molecular mechanisms of stacking fault formation in ice (I) and has implications for ice crystal growth phenomenology and the consequent physical and chemical properties of ice.

Materials properties, including thermal, mechanical, and electronic behavior, are dependent on the molecular arrangements at the nanoscale and can be strongly impacted by defects and/or dopants.[1−,3] In metal alloys, for instance, stacking faults formed as a result of dislocation evolution can affect plastic deformation of metal alloys,[2,4] and in alloys doped with impurities, the dopants segregate toward these stacking faults.[2] Hence, an understanding of the microscopic origins of defects and their formation is of fundamental importance for furthering our appreciation and mastery of materials. Hexagonal ice, the crystalline phase of water arising at atmospheric pressure, can be expected to contain defects that may sometimes cause a shift in the subsequent crystalline layers.[1,5] In an ice (I) crystal, these layer shifts can represent stacking faults that coincide with a cubic ice structure, a metastable form of ice (I).[1,6−14] Stacking faults in ice (I) are planar defects on the basal face of hexagonal ice or the (111) face of cubic ice that change the pattern of the layers between hexagonal and cubic stacking[1−8] (see SI-Figure 1). The origin of stacking faults within ice is currently believed to be either point defects,[1,9−13] which can be positional or orientational, or dislocations[5,14] in the crystal lattice formed during nucleation[6,15] or growth.[5,16−19] In this regard, fluctuations at the liquid−solid interface are an important factor in this process.[1,5−8,15] Point defects and dislocations can cause insertion or deletion (partial or complete) of layers of molecules[1,6,14] that distort the ideal hydrogen-bonding network in an ice lattice. Consequently, water molecules must reorganize themselves in attempting to satisfy their desire for four hydrogen bonds and to minimize void space in the presence of defects.[1,14,18,19] Depending on the nature of a defect, ice layers might shift with respect to each other, generating stacking faults. In current experimental investigations, it is rather difficult to track directly the phenomena leading to stacking fault formation because these events are prone to fluctuations if they occur at the interface and are otherwise beyond of the resolution of current instruments[5,7,12,14] if they persist below the growing layers. Molecular simulations can provide molecular-level insights into crystal growth phenomenology,[15,18,19] and we have utilized such an approach [see the technical details in the Supporting Information (SI)] to explore stacking fault formation during ice growth and characterize it microscopically.

Figures 1 and 2 show molecular configurations resulting from simulations of the directional growth of the basal (0001) and primary prism ($10\bar{1}0$) faces of hexagonal ice, respectively, from (undercooled) liquid water, where patterns associated with stacking faults are immediately observable. It is noteworthy that these molecular simulations of ice growth are the largest such reported to date. In both Figures 1 and 2, representative defective regions have been highlighted with color, and different cross-sectional slices of these defects are provided as additional panels. Two key features are common to all of the highlighted defective regions: the presence of two five-membered rings coupled to an eight-membered ring (5−8 rings) and the triangular character of the defective regions accommodating the stacking faults. The triangular morphology and its rough dimensions are comparable to the scanning tunneling microscopy (STM) images from a recent ice growth experiment[14] carried out at rather low temperatures (140 K).

Apart from the morphological similarities between the STM images and our results, the model proposed in ref 14 to account for the apparent occurrence of cubic ice layers in the STM experiment is similar to the molecular configurations presented in Figure 2b,d. However, this model is limited to the assumption that the apparent structural mismatches always occur at the positions of substrate steps, leading to formation of screw dislocations in the ice crystal. However, there are unexplained triangular features in the STM images[14] that appear to be associated with stacking faults that do not occur at step locations of the substrate. The phenomenology observed in the present work arises from the behavior of the ice itself, as there is no substrate. The coupled 5−8 ring defects, when viewed along the line of the defects as in Figure 2c, appear as stretched hexagonal cavities across the crystal and resemble the "voidlike" regions at grain boundaries (interfaces) sought by other groups[7] (also see SI-Figure 4). These coupled 5−8 ring defects not only facilitate stacking faults in an ice crystal but also can extend across a crystal,

Received: October 14, 2010
Published: December 29, 2010

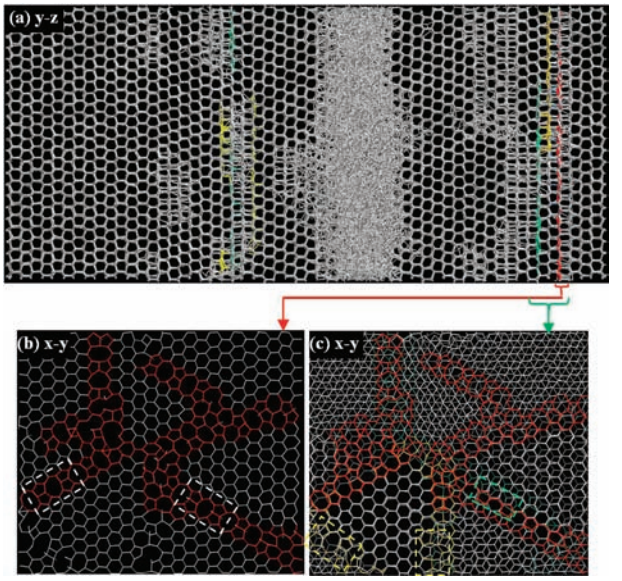

Figure 1. Defect structure in an ice−water system during directional growth of the basal face (0001) of hexagonal ice, I_h. This system configuration resulted from allowing ice to grow at 24 K undercooling for 35 ns; the direction of growth is defined as the *z* axis. (a) The *yz* projection of the final system, in which only hydrogen bonds between molecules are shown. Some representative defective regions are highlighted in red, yellow, or green. Panels (b) and (c) are single- and multilayer *xy* cross sections, respectively, of a representative defective region in the system. Coupled 5−8 ring motifs are highlighted with white rectangles in (b), whereas in (c) these features are highlighted with correspondingly colored rectangles. The apparent triangular morphology of the stacking fault regions in (b) and (c) is noteworthy. An alternative visualization of panel (c) is provided in SI-Figure 2. Additional *xy* cross-sectional slices are provided in SI-Figures 3 and 4.

which makes them a reasonable candidate for a structural motif present at (sub)grain boundaries.[7,20]

Although stacking faults are known as planar defects, their initiation is apparently a three-dimensional structural event. A possible mechanism is suggested in Figure 3, which illustrates that on the $(20\bar{2}1)$ face of hexagonal ice there are sets of 10-membered rings, a feature also shared by the (001) face of cubic ice. If two of the water molecules in these rings move inward and hydrogen bond (forming point defects) as pictured in Figure 3, then two five-membered rings result, one of which lies in the basal face and the other in the prism face. While five-membered rings are quite stable,[21] they interfere with further growth of the ice crystal. Additional water molecules in the face may adopt this pattern to form other pairs of five-membered rings, which are always separated by eight-membered rings. This motif then extends across an ice layer, producing a shift in the molecular positions of the next layer and hence a stacking fault. For a large (basal) interface, it is likely that an ice layer might nucleate as islands of crystals, which could grow until they reach each other's boundaries. If the stacking in these islands is not in register, then the coupled 5−8 ring defect could facilitate connecting the whole layer together (see SI-Figures 3 and 4).

There are other important factors in the observation of coupled 5−8 ring defects. One of these is the temperature. The degree of undercooling appears to be an essential factor in the appearance and stabilization of this defect. At smaller undercoolings (e.g., 15 K), the defect was rarely seen in our simulations, although experiments are still able to detect a noticeable

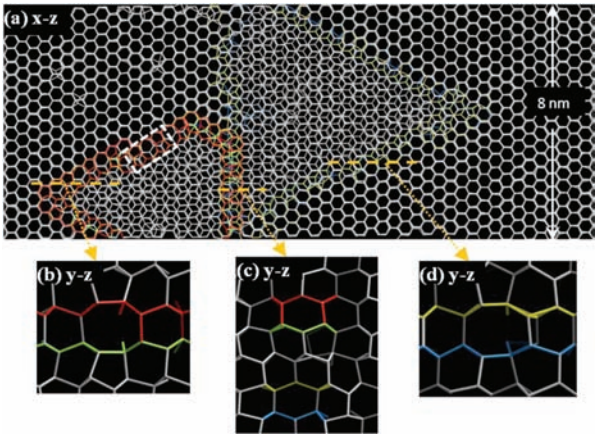

Figure 2. Defect structure in an ice−water system during directional growth of the primary prism face (10−10) of hexagonal ice, I_h. This system configuration resulted from allowing ice to grow at an undercooling of 24 K for 25 ns; the direction of growth is identified as the *z* axis. (a) The *xz* projection of the final system, in which only hydrogen bonds between molecules are shown. Within the grown ice crystal, four layers exhibiting defect motifs have been colored red, green, yellow, and blue from top to bottom in the direction of view. The triangular shape of the stacking faults resembles the patterns seen in the STM images in ref 9. Panels (b−d) are cross-sectional slices in the *yz* plane through the configuration, where coupled 5−8 ring defects are again apparent at the boundaries of the shifted layers. A representative defect has been highlighted in (a) by a white rectangle. An alternative visualization of panel (a) is provided in SI-Figure 5.

population of stacking faults.[12,13] It is expected that lower temperatures slow down annealing processes, thereby allowing for the survival of coupled five-membered rings. This is consistent with the STM experiment observations,[14] which were performed at low temperature; higher temperatures would likely have tended to anneal such defects in a growing ice crystal. It is the relatively low undercoolings and short observation times (relative to experimental observation and annealing times) of the present simulations that have aided in our observation of coupled 5−8 ring defects.

Periodic boundaries and the simulation length scale can also be important factors. Comparison of the defect features in Figures 1 and 2 with those shown in SI-Figures 6−9 indicates that smaller system size and lattice periodicity can easily constrain the defect either to anneal or to appear as part of a large feature. If a crystal cannot accommodate or anneal the defect, then further growth appears to stop (see SI-Figures 6 and 7). This supports the suggestion that previous workers had not detected coupled 5−8 ring defects or their morphological consequences because their systems were not of sufficient size to accommodate the necessary fluctuations.[15,18,19]

It is easy to envisage that solutes at an ice interface might be coupled to structural fluctuations and the formation of point defects[1] able to generate coupled 5−8 rings. In moderate-sized systems (i.e., those with widths of 2 to 3 nm), we observed that the presence of solutes such as methane, ammonia, and methylamine in the liquid phase can induce the formation of coupled 5−8 ring defects. Figure 4 presents representative examples that occurred during the directional growth of the (111) and (011) faces of cubic ice from an aqueous methane solution. The presence of methane molecules at the right time and place at the interface appeared to promote displacement of the appropriate water molecules to trigger five-membered ring formation

dx.doi.org/10.1021/ja109273m | *J. Am. Chem. Soc.* 2011, 133, 704–707

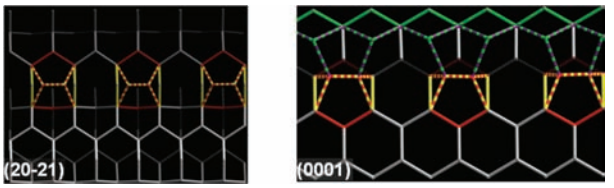

Figure 3. Formation of coupled 5−8 ring defects. The hydrogen-bonding network of water molecules is shown for the $(20\bar{2}1)$ and (0001) faces of hexagonal ice. The ideal (lattice) hydrogen bonds of a set of molecules that give rise to coupled 5−8 rings are colored solid red and yellow, whereas the defect-associated hydrogen bonds are depicted with yellow and red stripes. Hydrogen bonds that subsequently formed to complete the defect motif on the (0001) face are colored with purple and green stripes. The latter bonds formed instead of the (ideal) lattice bonds, which are colored green. The white lines represent the remainder of the ice-lattice hydrogen bonds. It can be seen that the formation of a hydrogen bond between two water molecules of a large 10-membered ring on the $(20\bar{2}1)$ face results in two coupled five-membered rings. One of these five-membered rings lies relatively flat in the (0001) face and the other one in the prism face. These coupled rings can help promote the formation of similar motifs in nearby lattice sites (green-and-purple-striped bonds) and can extend across the layer.

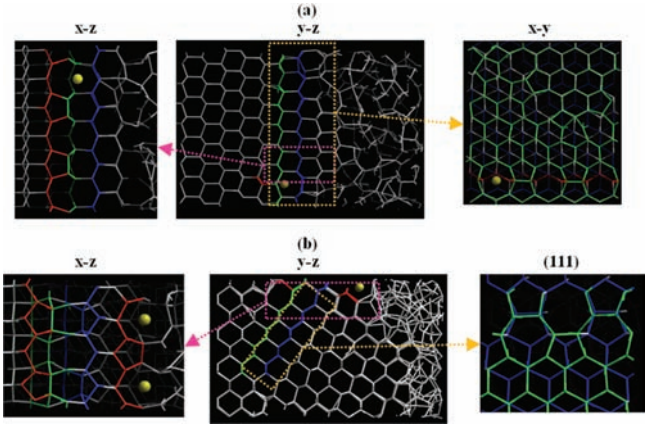

Figure 4. Defect structure in ice−water systems during directional growth of two faces of cubic ice, I_c, in the presence of a methane solute. Only the hydrogen bonds between water molecules are shown, and the yellow spheres represent methane molecules. The direction of ice growth is defined as the *z* axis. The defective layers are colored green and blue. Red water molecules have distorted hydrogen bonds to a defective layer and may have participated in formation of the defect. (a) System configuration resulting when the (111) face of cubic ice was allowed to grow from aqueous solution at an undercooling of 24 K for 37 ns. The left and right panels show slices through the system configuration along the *xz* and *xy* planes, respectively. An entrapped methane molecule can be seen to reside in proximity to an eight-membered ring structure. (b) System configuration resulting when the (011) face of cubic ice was allowed to grow from aqueous solution at an undercooling of 24 K for 43 ns. The green layer contains motifs of coupled 5−7 rings that apparently arise as a result of the structural mismatch with the layer containing the coupled 5−8 ring defect. The left panel presents the *xz* projection of the configuration, while the right panel provides a view of the coupled 5−8 ring defect on the (111) face.

(as demonstrated in Figure 3), leading to the defect. Specifically, it is the steric bulk of a methane molecule that increases the tendency of the two water molecules in a 10-membered ring on the (001) face of cubic ice or the $(20\bar{2}1)$ face of hexagonal ice to form a hydrogen bond (see Figure 4a). The resultant eight-membered ring pocket provides the methane molecule with an apparently favorable location to reside (stabilizing it in a manner not unlike that found in clathrate hydrate formation[22]). We should emphasize that as soon as these coupled 5−8 ring defects form on the (111) face of cubic ice or the (0001) face of hexagonal ice in moderate-sized systems, the growth of further ice layers effectively stops, as discussed above. The (011) face of cubic ice (see Figure 4b) also exhibited similar phenomenology in the presence of methane molecules. Other solutes, such as ammonia and methylamine, were also able to trigger the formation of coupled 5−8 rings (see the SI).

Along with coupled 5−8 ring defects, sets of coupled 5−7 rings[23] are also apparent in our configurations [Figure 1b,c; Figure 2a; Figure 4b (111); also see the SI]; these resemble Stone−Wales defects in graphene.[24] However, in graphene sheets, such 5−7 defects are strictly two-dimensional structures. Although coupled 5−7 rings in ice appear mainly in layers of hexagonal rings [Figure 1b; Figure 2a; Figure 4b (111)], they must have a three-dimentional nature because of the hydrogen-bonding network in ice. Furthermore, the presence of coupled 5−7 rings induces only a local intralayer perturbation (the rearrangement of a few molecules) in the ice structure,[23] which is incapable of inducing stacking faults. In contrast, coupled 5−8 ring defects engage multiple layers as they form (Figures 1 and 2) and thus facilitate stacking faults.

Apparently, the coupled 5−8 ring defect can provide a molecular basis for understanding a variety of experimental observations.[12,13] The characteristics of the coupled 5−8 ring defect, particularly the length scale of the resultant structures, match those of arrays of dislocations identified in ice cores,[5,12,13,20] which are evidently associated with (sub)grain boundaries. The density of these defects is apparently higher in our systems than estimates from experiments;[12] rapid growth rates and the lack of time for annealing are likely factors enhancing the appearance of coupled 5−8 defects in our simulations. Further structural, kinetic, and energetic aspects of this defect should clearly be investigated with approaches such as accurate ab initio simulations and spectroscopic techniques in conjunction with existing X-ray topographs of stacking faults[12] and STM images.[14] The role this defect can play in shifting ice layers to generate stacking faults, as well as its possible inclusion at (sub)grain boundaries, may help glaciologists[1,16] and planetary scientists[17,25,26] in interpreting the properties of defective ice crystals[27] formed under strain−stress or hydrostatic pressure conditions. It would assist atmospheric scientists[6] in understanding how impurities[5] may be incorporated into ice crystals and how they may affect the structure of ice. It may offer clues to cryobiologists[28,29] on how to prepare solutions from which ice (I) crystals with more cubic character might be produced; it is believed that such ice crystals would be smaller and less harmful to living tissues.[29] The presence of coupled five-membered rings accompanied by an eight-membered ring void may also provide the means for an ice surface to nucleate other structures, such as clathrate hydrates.[22]

■ ASSOCIATED CONTENT

Supporting Information. Simulation methods, complete ref 26, topology and stacking of hexagonal ice (0001) and cubic ice (111), additional cross-sectional slices for Figure 1, alternative visualizations of Figures 1c and 2a, and snapshots of other solutes inducing coupled 5−8 ring defects. This material is available free of charge via the Internet at http://pubs.acs.org.

AUTHOR INFORMATION

Corresponding Author
pkusalik@ucalgary.ca

ACKNOWLEDGMENT

The financial support of the NSERC and the University of Calgary is greatly appreciated. We are thankful for the computational facilities at Westgrid (www.westgrid.ca).

REFERENCES

(1) Petrenko, V. F.; Whitworth, R. W. *Physics of Ice*; Oxford University Press: New York, 2002.
(2) Schmidt, T. M.; Justo, J. F.; Fazzio, A. *J. Phys.: Condens. Matter* **2000**, *12*, 10235–10239.
(3) Kato, T.; Koyama, H.; Matsukawa, T.; Fujikawa, K. *Solid-State Electron.* **1976**, *19*, 955–959.
(4) Dudarev, E. F.; Kornienjo, L. A.; Bakach, G. P. *Russ. Phys. J.* **1991**, *34*, 207–216.
(5) Hondoh, T. In *Physics of Ice Core Records*; Hondoh, T., Ed.; Hokkaido University Press: Sapporo, Japan, 2000; pp 3−24.
(6) Murray, B. J.; Knopf, D. A.; Bertram, A. K. *Nature* **2009**, *434*, 202–205.
(7) Hansen, T. S.; Koza, M. M.; Kuhs, W. F. *J. Phys.: Condens. Matter* **2008**, *20*, No. 285104.
(8) Hansen, T. S.; Koza, M. M.; Lindner, P.; Kuhs, W. F. *J. Phys.: Condens. Matter* **2008**, *20*, No. 285105.
(9) de Koning, M.; Antonelli, A.; da Silva, A. J. R.; Fazzio, A. In *Physics and Chemistry of Ice*; Kuhs, W. F., Ed.; Royal Society of Chemistry: Cambridge, U.K., 2007; pp 155−161.
(10) de Koning, M.; Antonelli, A.; da Silva, A. J. R.; Fazzio, A. In *Physics and Chemistry of Ice*; Kuhs, W. F., Ed.; Royal Society of Chemistry: Cambridge, U.K., 2007; pp 163−169.
(11) Tsogbadrakh, N.; Morrison, I. In *Physics and Chemistry of Ice*; Kuhs, W. F., Ed.; Royal Society of Chemistry: Cambridge, U.K., 2007; pp 601−608.
(12) Baker, I. *Cryst. Growth Des.* **2002**, *2*, 127–134.
(13) Hondoh, T.; Itoh, T.; Amakal, S.; Goto, K.; Higashi, A. *J. Phys. Chem.* **1983**, *87*, 4040–4044.
(14) Thürmer, K.; Bartlet, N. C. *Phys. Rev. B* **2008**, *77*, No. 195425.
(15) Matsumoto, M.; Saito, S.; Ohmine, I. *Nature* **2002**, *416*, 409–413.
(16) Screen, J. A.; Simmonds, I. *Nature* **2010**, *464*, 1334–1337.
(17) Jewitt, D. C.; Luu, J. *Nature* **2004**, *432*, 731–733.
(18) Carignano, M. A. *J. Phys. Chem. C* **2007**, *111*, 501–504.
(19) Brukhno, A. V.; Anwar, J.; Davidchack, R.; Handel, R. *J. Phys.: Condens. Matter* **2008**, *20*, No. 494243.
(20) Weikusat, I.; Kipfstuhl, S.; Faria, S. H.; Azuma, N.; Miyamoto, A. *J. Glaciology* **2009**, *55*, 461–472.
(21) Belch, A. C.; Rice, S. A. *J. Chem. Phys.* **1987**, *86*, 5676–5682.
(22) Blake, D.; Allamandola, L.; Sandford, S.; Hudgins, D.; Freund, F. *Science* **1991**, *254*, 548–551.
(23) Grishina, N.; Buch, V. *J. Chem. Phys.* **2004**, *120*, 5217–5225.
(24) Ma, J.; Alfe, D.; Michealides, A.; Wang, E. *Phys. Rev. B* **2009**, *80*, No. 033407.
(25) Schenk, P. M. *Nature* **2004**, *417*, 419–421.
(26) Cuzzi, J. N.; et al. *Science* **2010**, *327*, 1470–1475.
(27) Han, Y. L.; Shokef, Y.; Alsayed, A. M.; Yunker, P.; Lubensky, T. C.; Yodh, A. G. *Nature* **2008**, *456*, 898–903.
(28) Mazur, P. *Science* **1970**, *168*, 939.
(29) Kohl, I.; Mayer, E.; Hallbrucker, A. *Phys. Chem. Chem. Phys.* **2000**, *2*, 1579–1586.